PSFC/JA-06-7

Measuring E and B fields in Laser-Produced plasmas with Monoenergetic Proton Radiography

C. K. Li,[1] R. P. J. Town,[2] F. H. Seguin,[1] S. P. Hatchett,[2] O. Landen,[2] J. A. Frenje,[1] R. Rygg,[1] A. Mackinnon,[2] J. P. Knauer,[3] T. C. Sangster,[3] V. Smalyak,[3] R. D. Petrasso[1]

1 June 2006

[1] Plasma Science and Fusion Center, Massachusetts Institute of Technology, Cambridge, Massachusetts 02139

[2] Lawrence Livermore national Laboratory, Livermore, California 94550

[3] Laboratory for Laser Energetics, University of Rochester, Rochester, New York 14623

The work described here was performed in part at the LLE National Laser User's Facility (NLUF), and was supported in part by US DOE (Grant No. DE-FG03-03SF22691), LLNL (subcontract Grant No. B504974), and LLE (subcontract Grant No. 412160-001G).

Accepted for publication in ***Physical Review Letters***

Measuring E and B fields in Laser-Produced Plasmas with Monoenergetic Proton Radiography

C. K. Li, F. H. Séguin, J. A. Frenje, R. Rygg, R. D. Petrasso
Plasma Science and Fusion Center, Massachusetts Institute of Technology, Cambridge, Massachusetts 02139

R. P. J. Town, P. A. Amendt, S. P. Hatchett, O. L. Landen, A. J. Mackinnon, P. K. Patel
Lawrence Livermore National Laboratory, Livermore, California 94550

V. A. Smalyuk, T. C. Sangster, J. P. Knauer
Laboratory for Laser Energetics, University of Rochester, Rochester, New York 14623

Electromagnetic (E/B) fields generated by the interaction with plasmas of long-pulse, low-intensity laser beams relevant to inertial confinement fusion have been measured for the first time using novel monoenergetic proton radiography methods. High-resolution, time-gated radiography images of a plastic foil driven by a 10^{14} W/cm^2 laser implied B fields of ~ 0.5 MG and E fields of ~ 1.5×10^8 V/m. Simulations of these experiments with LASNEX+LSP have been performed and are quantitatively consistent with the data both for field strengths and for spatial distributions; this is the first direct experimental test of the laser-generated B-field package in LASNEX. The experiments also demonstrated that laser phase plates substantially reduce small-scale chaotic field structure.

PACS numbers: 52.38 Fz, 52.50 Jm, 52.70. Nc

The generation of electromagnetic fields by interactions of laser light with matter is a process of fundamental interest in High-Energy-Density (HED) physics [1]. The primary mechanism behind field formation is the loss of energetic electrons from the heated region, resulting in the breakdown of neutrality. Many processes can then contribute to field generation and evolution, but their relative importance depends on interaction parameters [1-7]. For long-pulse, low-intensity laser light, the dominant source for B field generation is non-collinear electron density and temperature gradients ($\nabla n_e\times\nabla T_e$); the dominant source for E fields is $\nabla P/n_e$, a consequence of non-uniform laser irradiation [1-7]. For circular laser spots, the B fields have a toroidal configuration with scale length comparable to the spot size. In the regime with low Z and high temperature, where resistivity is low, B-field growth is usually linear in time and is balanced primarily by convective losses (*i.e.*, the B field is "frozen in") [1-3,6,7]. Under these circumstances, B field evolution can be described by the Faraday equation combined with a simplified version of the generalized Ohm's law,

$$\frac{\partial \mathbf{B}}{\partial t} \approx \nabla\times\left(\mathbf{v}\times\mathbf{B}\right) - \frac{1}{en_e}\nabla n_e\times\nabla T_e \quad , \tag{1}$$

where **v** is the plasma fluid velocity.

In addition to its importance to fundamental HED physics, these fields have important implications for several current problems. In inertial confinement fusion (ICF), for example, magnetic fields (~ MG) are generated inside a hohlraum by long-pulse (~ 1 ns) laser illumination [8-10]. Such fields can significantly reduce heat flow, since cross-field thermal conductivity is modified by a factor of $(1+\omega_{ce}^2\tau^2)^{-1}$, where ω_{ce} is the electron gyro frequency and τ is the collision time. The result is alteration in the distributions of electron temperature and density, enhancing laser-plasma instabilities and implosion asymmetries [8-10]. The experiments

described here are the first to directly measure fields generated by the types of laser beams used in direct- and indirect-drive ICF.

Previous work has focused largely on regimes in which fields are generated by short-pulse, high-intensity lasers [5,11-14], and field measurements were based on Faraday rotation [11,13] and probes [4], or high-order laser harmonics [14]. It has also been proposed that proton radiography could provide a different method for measuring these fields through the deflections they induce in proton trajectories; recent work by Mackinnon *et al*. [15] demonstrated that high-resolution images containing deflection information could be obtained, although no direct connections were made between images and fields. In their experiment, backlighter protons were generated by irradiating a solid tungsten target with a high-intensity petawatt laser beam (duration 300 fs with intensity 1×10^{19} W/cm^2); the result was a large proton flux and a continuous energy spectrum up to ~50 MeV. These protons were passed through a mesh and used to image a plasma generated by a single laser beam (300 ps) on a 120-μm Cu wire. More recently, work by Romagnani, *et al.* [16] utilized side-on proton radiography to study the E field generated by a high-intensity (~10^{18} W/cm^2), short-pulse (~1.5 ps) laser driving an Au foil. In their experiments, the probing proton flux had a continuous energy spectrum and was generated from a 10-μm Au foil irradiated by a laser pulse ~300 fs long at the intensity ~2×10^{19} W/cm^2.

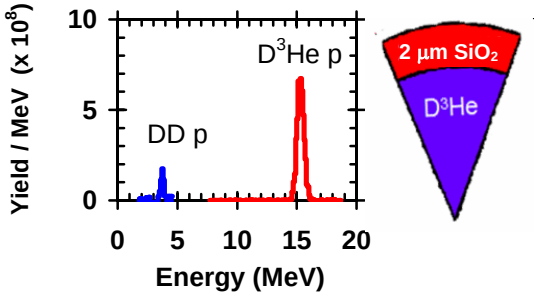

FIG. 1. Measured energy spectra of monoenergetic D^{3}He and DD protons generated in an implosion of a thin-glass shell filled with D^{3}He gas (OMEGA shot 42767). The data described in this Letter correspond to the D^{3}He protons; use of the 3-MeV DD protons will be explored in future work.

We recently developed a novel imaging technology that combines a monoenergetic proton backlighter with a matched detection system [17,18]. Protons are generated as nuclear fusion products from the reaction D+^{3}He→α+p in exploding-pusher implosions of D^{3}He-filled, glass-shell capsules [19]; the proton birth energy is E_p = 14.7 MeV, with a small amount of thermal broadening. For the experiments described here, the backligher implosions were driven by 20 OMEGA laser beams. A typical measured proton spectrum is shown in Fig. 1. The spatial size of the proton source was measured with a proton-emission imaging system [20], which determined that the source was nearly spherical and had approximately a Gaussian radial emission profile with 1/e radius ~ 27 μm. The timing of the proton production was measured by a proton temporal diagnostic (PTD) [21]; protons are produced during an interval of ~ 150 ps, and the time of onset of the burn was adjustable. The protons are detected by a CR-39 track detector configured for imaging [18]. This approach has distinct advantages over radiography with broad-band proton sources (such as intense-laser-induced sources); it allows us to optimize a special detector design and also to make precise connections between particle deflections and field magnitudes.

Our experimental setup, illustrated schematically in Fig. 2, was designed for quantitative imaging of fields generated by the interaction of a laser with a plastic (CH) foil. In each

individual experiment, 14.7-MeV backlighter protons were passed through meshes and used to simultaneously image two separate laser-plasma interactions; one was imaged face on, while the other was imaged from the side. The laser-plasma interactions on each CH foil were induced by a single laser beam (the *interaction beam*) with a wavelength of 0.351 μm and incident 23° from the normal direction. The laser had a square pulse either 1-ns or 0.6-ns long, with an energy of 500 J or 250 J. The diameter of the laser beam on the foil (containing 95% of the energy deposition) was determined by the phase plate, which was either SG2 (500 μm) or SG4 (800 μm) [22]; the resulting laser intensity was of order 10^{14} W/cm^2. X-ray emission indicate that the plasmas have $n_e \sim 10^{20}$-10^{22}/cm^3 and $T_e \sim 1$ keV. The experiments were modeled with the 2-dimensional LASNEX hydrocode [23], while the proton transport through the plasmas was modeled with the LSP hybrid PIC code [24]. Because only a single energy (14.7 MeV) was used, directly comparing simulations and experimental data provides unambiguous quantitative information about fields. Simulations [10] indicate that face-on radiography is largely sensitive only to the B field, while side-on radiography is primarily sensitive only to the E field. This allows E and B fields to be measured separately.

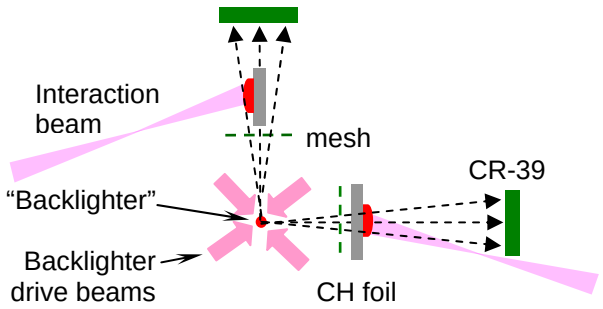

FIG. 2 Schematic illustration of our experiment setup and the physical relationship between the proton backlighter (imploded D^{3}He-filled capsule), mesh, CH foils, CR-39 imaging detectors, and OMEGA laser beams, as used for simultaneous radiography of two separate laser-foil interactions (face-on and side-on). The distances between backlighter and foil were about 1 cm, while the distances from foil to detector were 35 cm.

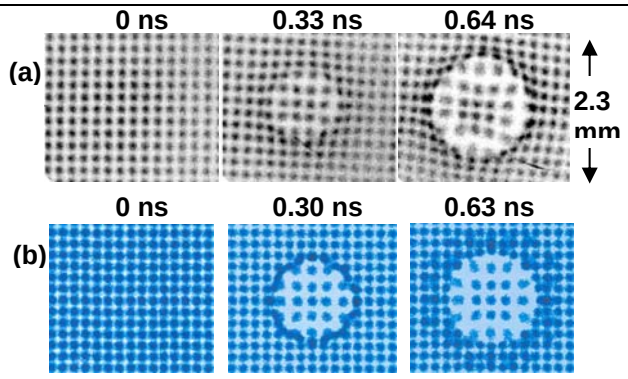

FIG. 3. (a) Measured face-on, 14.7-MeV-proton images showing the effects of the magnetic field generated by laser-plasma interactions. Each image is labeled by the time interval between the arrival at the foil of the interaction beam and the arrival of the imaging protons. The interaction beam had a 1-ns pulse length. (b) Images simulated by LASNEX+LSP for the conditions that produced the experimental images shown in (a). The vertical size of each image, scaled to the location of the foil, is about 2.3 mm.

Figure 3(a) shows the face-on images acquired from three different shots. The laser timing was adjusted so the 14.7-MeV protons arrived at the foil at 0.0, 0.33, and 0.64 ns, respectively, after the laser interaction beam was turned on. The laser beam had an SG4 phase

plate (diameter 800 μm), with a 1 ns pulse and 500 J of energy. The data agree quite well with the LASNEX+LSP simulations shown in Fig. 3(b), both in terms of the time dependence of the apparent diameter of the plasma bubble and in terms of the amount of distortion of the mesh pattern inside the plasma bubble region due to the magnetic lens effect; this indicates that the relevant physics issues were properly addressed in the simulations. Significant distortions occurred near the border of the bubble, where the proton beamlets were deflected by a strong B field and piled up to form a sharp circular ring; smaller distortion at the center indicates a smaller, but measurable B field there. These features are confirmed by simulations illustrated in Fig. 4, showing that toroidal B fields are concentrated on a hemispherical shell surrounding the ablative plasma bubble; they have maximum amplitude near the edge but fall to zero at the center. The experimental images also show a slight mesh distortion outside the laser spot that is not apparent in the simulations. This could suggest that the simulations underestimated the plasma resistivity, or that the interaction laser had more energy in its wings than assumed in the simulations. We are able to estimate the B fields from the data by using the deflection of the beamlets from where they would be in an image without the distortion (ξ), together with the geometry of the imaging system and the scale length ($L_B \equiv B/\nabla B$) in the direction perpendicular to the image ($B \propto \xi E_p^{0.5} L_B^{-1}$). L_B was estimated approximately: $L_B \sim L_{\|} \equiv n_e/\nabla n_e$, which is about the radius of the plasma bubble. This estimated L_B is within a factor of 2 of what one would infer from the simulations near the edge of the bubble. The inferred peak B values of about 0.5 MG agree well with simulations. In contrast to previous experiments and simulations, where the plasmas were usually generated by a short-pulse laser (~1 to 100 ps), we used long pulses which result in time evolution on a scale longer that our 150-ps sampling time; this allows us to clearly measure the time evolution of the field structure as shown in Fig. 3.

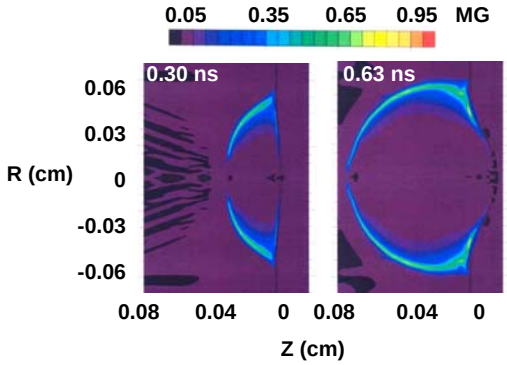

FIG. 4. Time evolution of B field strength on a cross section of the plasma bubble, simulated by LASNEX for the experimental conditions of Fig. 3. In each case, the horizontal coordinate z is distance from the foil (assuming the laser is incident from the left) and the vertical coordinate *R* is distance from the central axis of the plasma bubble. The largest field occurs near the surface of the plasma bubble, and the largest line integral parallel to the z direction occurs near the radial position of the bubble edge.

Images acquired with different phase plates are contrasted in Fig. 5: SG4 for the first row (800 μm) and SG2 for the second row (500 μm). In all cases the laser pulses had similar energy and pulse shape (~250J, 0.6-ns square), so the laser intensity for the second row was ~2.6 times higher; this resulted in about twice the image distortion, corresponding to a B field about twice as large. A larger deflection is measured in the center region for SG2 than for SG4 at ~0.4 ns, but not at ~0.7 ns. This is consistent with our LASNEX simulations, which show that significant B field is generated in the central region at earlier times, but that it moves to the edge of the plasma due to the plasma expansion.

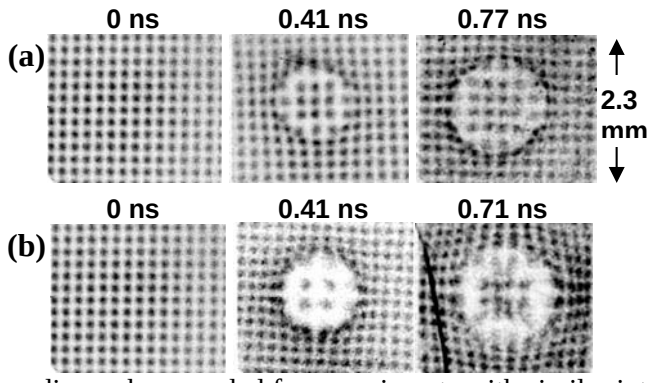

FIG. 5. 14.7-MeV-proton radiographs recorded for experiments with similar interaction laser pulse (~0.6 ns square, ~250 J) but different phase plates: (a) SG4 and (b) SG2. The smaller diameter of the SG2 beam resulted in an intensity 2.6 times higher than SG4, causing greatly increased image distortion.

The two images shown in Fig. 6 show a consequence of using no phase plate for the interaction beam. Both images were recorded around 0.3 ns, and utilized similar interaction beam diameters, pulse shapes and laser energy. The image recorded without phase plate [Fig. 6(b)] shows a pattern that is significantly more chaotic, containing a B field component with small-scale structure (~20-30% of the bubble size). Several physical mechanisms may contribute to the generation of these small-scale, random structures, in particular those associated with very localized regions of strong $\nabla n_e \times \nabla T_e$, including the resonance absorptions at local oblique incidence, filaments, laser hot spots, and instabilities [1-7]. Use of phase plates [Fig. 6(a)] eliminates the small-scale structure.

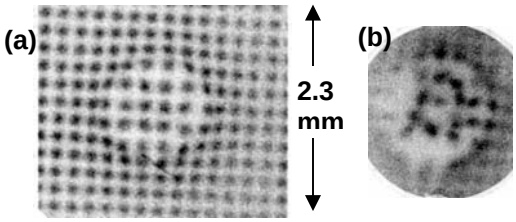

FIG. 6. Effects of phase plates on B-field structure is demonstrated by 14.7-MeV proton radiographs made using interaction beams with (a) and without (b) phase plates under conditions otherwise similar. [image (b) is from an earlier experiment in which the field of view was smaller and the outer (gray) part of the imaged area was covered by a 70-μm mylar washer]. Chaotic structure is clearly seen in image (b)

Side-on measured (a) and simulated (b) images are shown in Fig. 7 for the same shot that generated the center image shown in Fig. 5 (b). The displacements of the beamlets away from the foil represent the effect of an electric field perpendicular to the foil. The size of the apparent beamlet displacement ($\xi \approx 60$ μm) is used to estimate the E field strength ($E \propto \xi E_p L_\perp^{-1}$); by assuming that the field operates over a scale length $L_\perp$ comparable to the radius of the plasma bubble, $E \approx 1.5\times10^8$ V/m was deduced. The magnitude of the beamlet displacement in the experiment is very similar to what is seen in the simulation.

In summary, we studied electromagnetic fields generated by the interaction with plasmas of long-pulse, low-intensity laser beams that are particularly relevant to inertial confinement fusion experiments. The field strengths have been measured using novel monoenergetic proton radiography methods. High-resolution, time-gated radiography images of a plastic foil driven by a 10^{14} W/cm^2 laser implied B fields of ~ 0.5 MG and E fields of ~ 1.5×10^8 V/m. Simulations of these experiments with LASNEX+LSP are quantitatively consistent with the data for both field

strengths and spatial distributions and confirm experimentally, for the first time, the accuracy of the B-field generation package in LASNEX. The experiments also demonstrated the smoothing effects of laser phase plates by showing that they substantially reduce small-scale chaotic field structure.

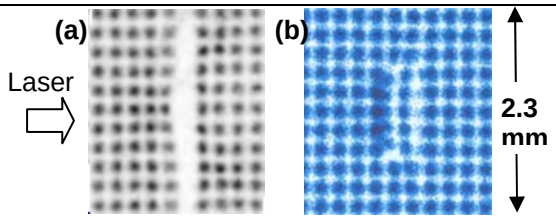

FIG. 7. Data (a) and simulation (b) for the side-on images. The distortion in the center column of (a) resulted from the E field. The large separation between the two center columns of beamlets in (a) is due to attenuation by the CH foil, which is 50 μm thick but 3 mm long in the direction parallel to the proton trajectories; this effect is not seen in (b) because proton-foil interactions were not modeled in the LSP simulation. The magnitude of the beamlet displacement in the experiment is very similar to what is seen in the simulation.

The work described here was performed in part at the LLE National Laser User's Facility (NLUF), and was supported in part by US DOE (Grant No. DE-FG03-03SF22691), LLNL (subcontract Grant No. B504974), and LLE (subcontract Grant No. 412160-001G).

[1] S. Eliezer, *The Interaction of High-Power Lasers with Plasmas* (IOP Publishing Ltd. Bristol and Philadelphia, 2002).
[2] L. Spitzer, *Physics of Fully Ionized Gases* (Interscience, New York, 1962).
[3] S. I. Braginskii, *Review of Plasma Physics* 1 (Consultants Bureau, New York, 1965).
[4] J. A. Stamper *et al.*, Phys. Rev. Lett. **26,** 1012 (1971).
[5] D. G. Colombant *et al.*, Phys. Rev. Lett. **38,** 697 (1977).
[6] A. Nishiguchi *et al.*, Phys. Rev. Lett. **53,** 262 (1984).
[7] M. G. Haines, Phys. Rev. Lett. **78,** 254 (1997).
[8] S. H. Glenzer *et al.*, Phys. Rev. Lett. **87**, 045002 (2001).
[9] P. A. Amendt *et al.*, Bull. Am. Phys. Soc. **49**, 26 (2004).
[10] R. P. J. Town *et al.*, Bull. Am. Phys. Soc. **50**, 123 (2005).
[11] A. Raven *et al.*, Phys. Rev. Lett. **41,** 554 (1978).
[12] M. A. Yates *et al.*, Phys. Rev. Lett. **49,** 1702 (1982);
[13] M. Borghesi *et al.*, Phys. Rev. Lett. **81**, 112 (1998).
[14] U. Wagner *et al.*, Phys. Rev. E **70**, 026401 (2004).
[15] A. J. Mackinnon *et al.*, Rev. Sci. Instrum. **75**, 3531 (2004).
[16] L. Romagnani, *et al.*, Phys. Rev. Lett**. 95,** 195001 (2005).
[17] C. K. Li *et al.*, accepted for publication in Rev. Sci. Instrum. (2006)
[18] F. H. Séguin *et al.*, Rev. Sci. Instrum. **74**, 975 (2003).
[19] C. K. Li *et al.*, Phys. Plasmas **7**, 2578 (2000).
[20] F. H. Séguin *et al.*, Rev. Sci. Instrum. **75**, 3520 (2004).
[21] J. A. Frenje *et al.*, Phys. Plasmas **11**, 2480 (2004).
[22] F. J. Marshall *et al.*, Phys. Plasmas **11**, 251 (2004).
[23] G. B. Zimmerman and W. L. Kruer, Comments in Plasma Physics and Controlled Fusion **2**, 51 (1975).
[24] D. R. Welch, *et al.*, Nucl. Inst. Meth. Phys. Res. A **464**, 134 (2001).